

## **Next-generation Surface Enhanced Raman Scattering (SERS) Substrates for Hazard Detection**

**by Mikella E. Farrell, Ellen L. Holthoff and Paul M. Pellegrino**

**ARL-RP-0411**

**September 2012**

*A reprint from SPIE Defense and Security, 23 April 2012*

## **NOTICES**

### **Disclaimers**

The findings in this report are not to be construed as an official Department of the Army position unless so designated by other authorized documents.

Citation of manufacturer's or trade names does not constitute an official endorsement or approval of the use thereof.

Destroy this report when it is no longer needed. Do not return it to the originator.

# **Army Research Laboratory**

Adelphi, MD 20783-1197

---

**ARL-RP-0411****September 2012**

---

## **Next-generation Surface Enhanced Raman Scattering (SERS) Substrates for Hazard Detection**

**Mikella E. Farrell, Ellen L. Holthoff and Paul M. Pellegrino**  
**Sensors and Electron Devices Directorate, ARL**

*A reprint from SPIE Defense and Security, 23 April 2012*

REPORT DOCUMENTATION PAGE			Form Approved OMB No. 0704-0188		
<p>Public reporting burden for this collection of information is estimated to average 1 hour per response, including the time for reviewing instructions, searching existing data sources, gathering and maintaining the data needed, and completing and reviewing the collection information. Send comments regarding this burden estimate or any other aspect of this collection of information, including suggestions for reducing the burden, to Department of Defense, Washington Headquarters Services, Directorate for Information Operations and Reports (0704-0188), 1215 Jefferson Davis Highway, Suite 1204, Arlington, VA 22202-4302. Respondents should be aware that notwithstanding any other provision of law, no person shall be subject to any penalty for failing to comply with a collection of information if it does not display a currently valid OMB control number.</p> <p><b>PLEASE DO NOT RETURN YOUR FORM TO THE ABOVE ADDRESS.</b></p>					
1. REPORT DATE (DD-MM-YYYY) September 2012		2. REPORT TYPE Reprint		3. DATES COVERED (From - To)	
4. TITLE AND SUBTITLE Next-generation Surface Enhanced Raman Scattering (SERS) Substrates for Hazard Detection			5a. CONTRACT NUMBER		
			5b. GRANT NUMBER		
			5c. PROGRAM ELEMENT NUMBER		
6. AUTHOR(S) Mikella E. Farrell, Ellen L. Holthoff and Paul M. Pellegrino			5d. PROJECT NUMBER		
			5e. TASK NUMBER		
			5f. WORK UNIT NUMBER		
7. PERFORMING ORGANIZATION NAME(S) AND ADDRESS(ES) U.S. Army Research Laboratory ATTN: RDRL-SEE-E 2800 Powder Mill Road Adelphi, MD 20783-1197			8. PERFORMING ORGANIZATION REPORT NUMBER ARL-RP-0411		
9. SPONSORING/MONITORING AGENCY NAME(S) AND ADDRESS(ES)			10. SPONSOR/MONITOR'S ACRONYM(S)		
			11. SPONSOR/MONITOR'S REPORT NUMBER(S)		
12. DISTRIBUTION/AVAILABILITY STATEMENT Approved for public release; distribution unlimited.					
13. SUPPLEMENTARY NOTES					
14. ABSTRACT <p>Sensitive, accurate and reliable methods are needed for the detection and identification of hazardous materials (chemical, biological, and energetic) in the field. Utilizing such a sensing capability incorporated into a portable detection system would have wide spread beneficial impact to the U.S. military and first responder communities. Surface enhanced Raman scattering (SERS) is increasingly becoming a reputable technique for the real-time, dynamic detection and identification of hazard materials. SERS is particularly advantageous as it does not suffer from interferences from water, requires little to no sample preparation, is robust and can be used in numerous environments, is relatively insensitive to the wavelength of excitation employed, and produces a narrow-band spectral signature unique to the molecular vibrations of the analyte.</p> <p>We will report on the characterization and sensing capabilities of these next generation SERS substrates for the detection of energetic materials (ammonium nitrate, TNT, PETN, and RDX). Additionally, new efforts producing highly uniform samples, with known concentrations of energetic materials inkjet printed onto the SERS sensing surface using a precisely calibrated MicroJet system will be shown.</p>					
15. SUBJECT TERMS SERS, sensor, chemical, biological, energetic, Raman, detection, ammonium nitrate					
16. SECURITY CLASSIFICATION OF:			17. LIMITATION OF ABSTRACT  UU	18. NUMBER OF PAGES  16	19a. NAME OF RESPONSIBLE PERSON Mikella E. Farrell
a. REPORT UNCLASSIFIED	b. ABSTRACT UNCLASSIFIED	c. THIS PAGE UNCLASSIFIED			19b. TELEPHONE NUMBER (Include area code) (301) 394-0948

# Next generation Surface Enhanced Raman Scattering (SERS) substrates for Hazard Detection

Mikella E. Farrell, Ellen L. Holthoff and Paul M. Pellegrino

U.S. Army Research Laboratory  
RDRL-SEE-E  
2800 Powder Mill Rd.  
Adelphi, MD 20783

## ABSTRACT

Sensitive, accurate and reliable methods are needed for the detection and identification of hazardous materials (chemical, biological, and energetic) in the field. Utilizing such a sensing capability incorporated into a portable detection system would have wide spread beneficial impact to the U.S. military and first responder communities. Surface enhanced Raman scattering (SERS) is increasingly becoming a reputable technique for the real-time, dynamic detection and identification of hazard materials. SERS is particularly advantageous as it does not suffer from interferences from water, requires little to no sample preparation, is robust and can be used in numerous environments, is relatively insensitive to the wavelength of excitation employed, and produces a narrow-band spectral signature unique to the molecular vibrations of the analyte.

We will report on the characterization and sensing capabilities of these next generation SERS substrates for the detection of energetic materials (ammonium nitrate, TNT, PETN, and RDX). Additionally, new efforts producing highly uniform samples, with known concentrations of energetic materials inkjet printed onto the SERS sensing surface using a precisely calibrated MicroJet system will be shown.

**KEYWORDS:** SERS, sensor, chemical, biological, energetic, Raman, detection, ammonium nitrate

## I. INTRODUCTION

As of early 2012, the world population was estimated to have increased to around 7 billion people. It is anticipated that between 50 and 70 million people will be added annually to the world population until the mid 2030s.<sup>(1)</sup> To feed this ever increasing population and demonstrate healthy economic growth, agricultural industries since the 1900's have relied on manufactured fertilizers to increase their agricultural output. One ubiquitous fertilizer component is ammonium nitrate (AN). Ammonium nitrate is a solid fertilizer (~ 34 % nitrogen) typically applied and distributed in a solid prilled form. Nitrogen-based fertilizers account for almost 97% of the fertilizers used in agriculture.<sup>(2)</sup> The forecast is for world nitrogen fertilizer demand to increase at an annual rate of about 1.4% until 2011/2012, which is an overall increase of 7.3 million tons.<sup>(1)</sup>

While AN has many practical applications in agriculture, it is also extensively used in the manufacture of industrial explosives. One common industrial use of AN is in the fabrication of ammonium nitrate fuel oil or ANFO-based explosives. A typical ANFO consists of 84% prilled ammonium nitrate that acts as an oxidizing agent and absorbant for fuel.<sup>(2)</sup> While there are many examples of AN being used in industry, unfortunately it is also becoming a regularly used and almost established component of fertilizer bombs or improvised explosive devices (IEDs) seen throughout the world. One tragic example of terrorist use of AN occurred in the attacks in the US in 1995 with the bombing of the Alfred P. Murrah Federal Building in downtown Oklahoma City.<sup>(3)</sup> Since then, the use of AN by terrorist groups and the resulting devastation from material detonation, has continued to challenge military and law enforcement personnel both at home and abroad. In 2012, USA Today reported<sup>(4)</sup> that in Afghanistan the "number of improvised explosive devices that were cleared or detonated rose to 16,554 from 15,225, an increase of 9%." With the evident increase in IEDs and easily obtained and prevalent supply of ammonium nitrate in agricultural areas, the US Army and first responder community

are increasingly focusing efforts on energetic materials detection and identification.<sup>(5-13)</sup> Analytes of interest include both energetic materials and commonly used components in IEDs.<sup>(14-16)</sup>

There are several examples of laser-based systems that were designed to allow rapid detection and identification of hazardous materials.<sup>(17)</sup> Many of these systems offer standard detection capabilities on new sensing platforms, like vehicle and man portable systems. Of the many available standoff techniques researched for energetic and hazardous materials detection, some that are gaining growing attention are Raman and Raman-based technologies.<sup>(18-23)</sup> Raman and Raman-based techniques are increasingly being used to address the outstanding need and challenge for rapid, sensitive, accurate detection, identification, and quantification of chemical, biological, and energetic hazards in many fields of interest (e.g., medical, environmental, industrial, and defense applications).<sup>(24)</sup> In particular, there has been a push to detect trace levels of hazardous materials left behind on common items like hair, clothes, and even fingerprints.

One spectroscopic detection method that is gaining significant popularity for meeting these sensitivity needs is surface enhanced Raman scattering (SERS). SERS-based techniques and platforms combine traditional spectroscopy with trace level detection capabilities. SERS is particularly advantageous and an appropriate detection technique to utilize for hazard detection as it does not suffer from interferences from water, requires little to no sample preparation, is robust and can be used in numerous environments, is relatively insensitive to the wavelength of excitation employed and produces a narrow-band spectral signature unique to the molecular vibrations of the analyte.

Since the discovery of SERS in the 1970's, it has been experimentally shown that the SERS signal enhancements are typically observed on metalized (typically silver or gold) nanoscale roughened surfaces.<sup>(25-27)</sup> In the SERS literature, the two mechanisms that have been shown to control the enhancement of the Raman scattering (SERS) are considered to be the electromagnetic fields generated at or near nanoparticle surfaces and the physical (chemical) adsorption of a target analyte onto a surface.<sup>(28-31)</sup> The electromagnetic enhancement (EM) is typically deemed to be the stronger contribution, with an enhancement factor (as compared to spontaneous Raman) ranging from approximately  $10^4$  to  $10^{14}$ ,<sup>(32)</sup> while the chemical enhancement (CE) has been suggested to contribute at most  $10^2$ .<sup>(33)</sup> Because of the many sensing advantages of SERS-based techniques, significant research efforts (defense, industrial and academic) have been directed toward developing SERS substrates for SERS-based sensor platforms.<sup>(33-42)</sup>

Due to the many advantages offered by SERS, there has been an intense research push to fabricate "better" SERS sensing platforms. Some of these SERS platforms are fabricated from colloids<sup>(43)</sup>, film over nanospheres<sup>(44-47)</sup>, fiber optic bundles<sup>(48)</sup>, nanoparticles,<sup>(40, 49-52)</sup> and lithographically<sup>(53)</sup> produced structures. At best, typically the more sensitive substrate platforms generally have a 15% relative standard deviation (RSD; the measure of the reproducibility of an analysis) from substrate-to-substrate and SERS signal enhancements of 7 to 8 orders of magnitude.<sup>(45, 46)</sup> Consequently, many researchers in academia, industry, and government have focused concerted efforts toward increasing the signal enhancement ability, reproducibility, and mass production manufacturing of substrates to increase the utility of this technique.<sup>(53, 54)</sup> For the Army and first responders, such a substrate platform with increased sensitivity and reliability would be very advantageous for the detection and identification of unknowns.<sup>(55, 56)</sup>

Significant research efforts have also been concentrated on better directing the optimization of the substrate surface from which the SERS enhancement occurs.<sup>(53, 57-60)</sup> Based in part on experimental and theoretical efforts, the directed fabrication of SERS platforms has focused on modifying the feature size<sup>(61-63)</sup>, spacing between objects, geometry and shape of structures<sup>(64-66)</sup>, identity and incorporation of metals on the surface<sup>(67)</sup>, feature height, and the character of the foundation layer<sup>(44, 68-70)</sup> on which the architecture is fabricated.<sup>(56, 71, 72)</sup> There are numerous examples in the literature detailing how variation in some of these parameters in certain cases can result in very dramatic changes to the overall SERS enhancing capabilities of the substrate surface. Rigorous efforts continue to focus on developing an understanding about how these parameters can synergistically work together to result in a highly reproducible and sensitive SERS substrate. As focus continues on improving the overall sensing capabilities of the SERS surface, congruently research continues to push towards the development of a uniform reproducible mass produced platform necessary to facilitate widespread incorporation of SERS in viable sensing platforms.

Some success fabricating both spectrally and physically reproducible SERS substrates has been demonstrated with commercially available standard Klarite™ substrates (Renishaw Diagnostics).<sup>(58, 73-76)</sup> These substrates were developed using Silicon-based semiconductor fabrication techniques.<sup>(76)</sup> Klarite substrates are fabricated using a well defined

silicon fabrication technique in which a silicon diode mask is defined by optical lithography, and then potassium hydroxide (KOH) surface etched. The process results in an array of highly reproducible inverted pyramid features.<sup>(76)</sup> These array pyramids are reported to have “hot spots” or “trapped plasmons” located inside the wells.<sup>(76)</sup> These substrates have been previously characterized.<sup>(77)</sup> Atomic force microscopy (AFM) images have demonstrated that the inverted pyramid features are about 1.47  $\mu\text{m}$  in width and 1  $\mu\text{m}$  in depth. These substrates have plasmon absorbance bands located at 577 nm and 749 nm, thus demonstrating the usefulness of this substrate for a range of excitation sources. Additionally, due to the fabrication process used, under ideal conditions these substrates have demonstrated typical RSDs ranging from 10-15% under drop and dry conditions. While these standard Klarite substrates do demonstrate a high degree of substrate reproducibility and very low substrate background (SERS signal and surface morphology), for many applications to real-world situations, increased analyte sensitivity is still necessary. Recently new prototype Klarite based substrates have been fabricated by Renishaw Diagnostics with the intent to expand substrate sensing capabilities. The morphologies of these substrates dramatically differ in overall shape, pitch and spacing as compared to the standard Klarite substrate, resulting in very interesting sensing capabilities.<sup>(78, 79)</sup>

In this proceedings paper, preliminary efforts characterizing energetic materials deposited onto commercially available SERS substrates will be discussed and demonstrated. These hazard materials are deposited at low concentrations, serving as a proof of principle demonstration for future application for trace detection. By demonstrating these preliminary results, the potential of these SERS substrates for future incorporation in fielded Raman systems for the sensing of hazard materials can be imagined.

## II. EXPERIMENTAL

*Chemicals and Reagents.* All chemicals were used as received without further purification. The common chemical ammonium nitrate (AN) was used as received from Sigma. The energetic samples 1,3,5-trinitro-1,3,5-triazine (RDX), trinitrotolulene (TNT) and pentaerythritol tetranitrate (PETN) were obtained from Cerilliant (10 mg/mL, 99.9% purity). All inkjet printer stock solutions were prepared in acetonitrile or a water and methanol containing solution.

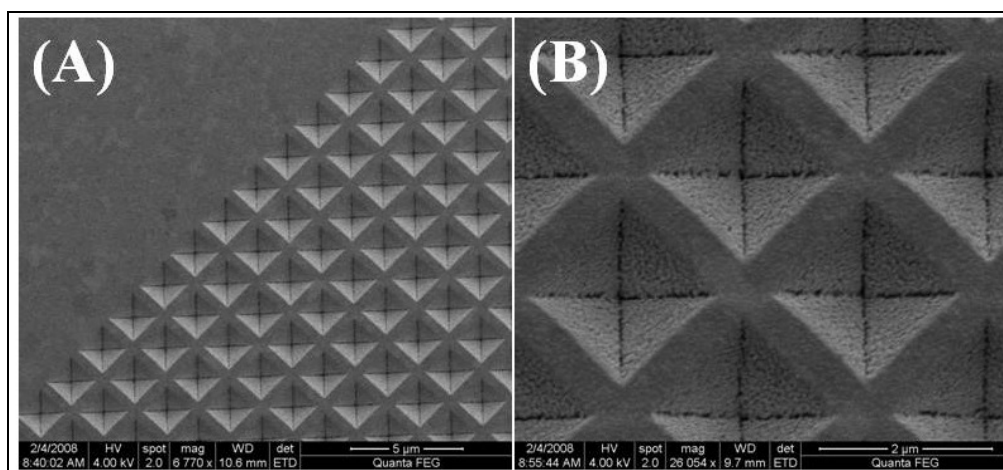


Figure 1. SEM data for the standard Klarite substrate as shown at two different magnifications. In (A) the active area is shown with the features and inactive area appears smooth. In (B) a higher magnification SEM image of the features of the substrate are shown.

*Commercially available substrates.* Commercially available slide mounted standard Klarite™ 302 SERS substrates were purchased from Renishaw Diagnostics. Slides were individually wrapped and vacuum sealed. The SERS active area on these slides is a small 4 mm x 4 mm wafer with a gold surface. The standard Klarite™ slides were only used once and opened just prior to measurement to reduce any possible surface fouling. Additionally, the substrate was submerged in ethanol to remove any possible contamination that may have accumulated on the surface. Next generation Klarite substrates (designated as 308's) were used as received from Renishaw Diagnostics following the same procedures used for the standard substrates. Most data in this proceedings paper will be presented as an average of a collected data set

and the standard deviation error shown, unless otherwise indicated. See Figure 1 for an example SEM image of a typical Klarite standard SERS substrate.

#### *Instrumentation and Data Analysis.*

Scanning electron microscope (SEM) images was obtained using a FEI environmental SEM (Quanta 200 FEG).

A Renishaw inVia Reflex Raman microscope was used for SERS and Raman spectra collection. Spectra were collected using a 785 nm laser. The laser light was focused onto the sample using a 5X objective, exposures were 10 seconds in length, and 3 accumulations were collected per spot. Approximately 7 mW of power irradiated the surface of the substrate. Five spectra were collected from each substrate. Samples were positioned using a motorized XYZ translational stage internal to the microscope. Spectra were collected, and the instrument was run using Wire 3.2 software operating on a dedicated computer. Data analysis was achieved using IgorPro 6.0 software (Wavemetrics).<sup>(78)</sup>

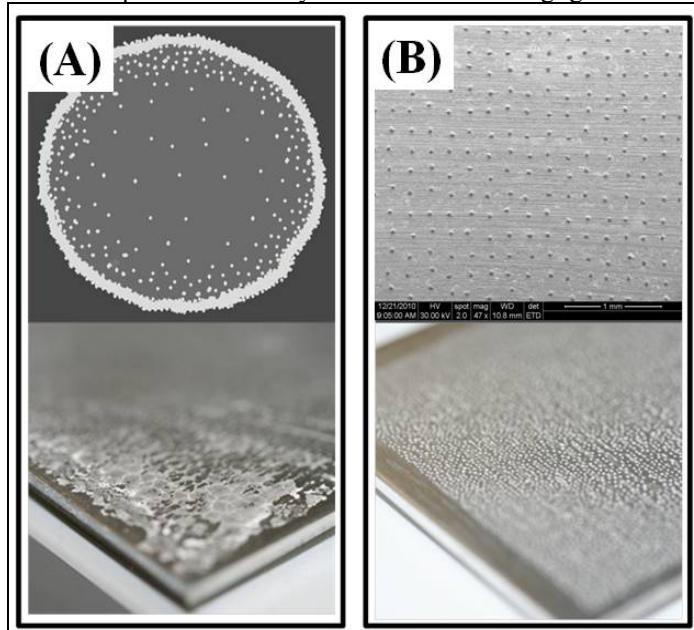


Figure 2. Example images from drop and dry and microjetted samples. (A) Graphic and photograph of drop and dry sample deposition demonstrates uneven dispersion and the coffee ring effect. (B) SEM image and photograph of an array of microdroplets demonstrates a more even sample dispersion when sample is dispensed with the microdispenser.

*MicroFab Technologies Printer.* Materials were produced using a JetLab<sup>®</sup> 4 (MicroFab Technologies) tabletop printing platform and have been previously documented.<sup>(80)</sup> Briefly, the JetLab<sup>®</sup> 4 is a drop-on-demand inkjet printing system with drop ejection drive electronics (JetDrive<sup>™</sup> III), pressure control, a drop visualization system, and precision *X*, *Y*, *Z* motion control. The dispensing device (print head assembly, MJ-AL-01-060) consists of a glass capillary tube, with a 60  $\mu\text{m}$  diameter orifice coupled to a piezoelectric element. Voltage pulses (20–25 V; rise time 1  $\mu\text{s}$ ; dwell time 28–32  $\mu\text{s}$ ; fall time 1  $\mu\text{s}$ ) applied to the piezo result in pressure fluctuations around the capillary. These pressure oscillations propagate through the printing fluid in the tube, resulting in ejection of a microdrop. Drops are visualized using synchronized strobe illumination and a charged coupled device (CCD) camera. Determining optimal jetting parameters is a trial-and-error process. Stable droplet ejection is achieved by visually observing expelled microdrops and adjusting voltage pulse parameters and capillary fluid backfill pressure. Conditions that provide the highest drop velocity without satellite droplet formation are desired. Printing was performed at a frequency of 250 Hz with a droplet velocity of  $\sim 2$  m/s. Drop diameter was estimated to be  $\sim 60$   $\mu\text{m}$ , based on the capillary orifice diameter. During printing, a single substrate was placed on the sample stage. The print head remained fixed at a specified height while the stage moved to print a specified pattern. A rectangular array, which covers a rectangular area with rows of equidistant points, was pre-programmed based on the substrate size and desired sample concentration. An array pattern was chosen for the purpose of creating the effect of a homogeneous coating for optical interrogation. Depending on the desired concentration per unit area (e.g.,  $\mu\text{g}/\text{cm}^2$ ), the total number of drops needed to achieve the desired concentration in that area was calculated



based on the mass of a single microdrop. Based on the number of total drops needed, the array spacing and drops needed per line can be calculated. These values are easily adjusted depending on concentration. Arrays were printed using the print on-the-fly mode. In this mode, the stage moves continuously as a single microdrop is dispensed at each array element. Print on-the-fly mode improves sample throughput.

### III. RESULTS AND DISCUSSION

Using the microjetting system, the analyte ammonium nitrate (AN) was jetted onto standard Klarite substrates at differing concentrations ranging from 0.05  $\mu\text{g}/\text{cm}^2$  to 50  $\mu\text{g}/\text{cm}^2$ . These concentrations were independently validated by UV-Vis measurements (data not shown), and have been previously discussed.<sup>(80)</sup> This concentration range was initially chosen as a proof-of-principle demonstration to determine if the AN could be detected via SERS and validate that there was a change on overall SERS signal intensity with an increase in analyte concentration on the standard Klarite substrate. In Figure 3, some example SEM images (A-D) and a typical spectrum for AN are shown (E). In the SEM images in Figure 3 A and B, the images of the AN droplet physically appear dramatically different, (A) is smooth while (B) appears to have a faceted structure. It has previously been observed that at varying concentrations (trace vs. bulk) different phases of energetic materials can exist,<sup>(8, 21, 23, 81)</sup> however, this discussion is beyond the scope of this proceedings paper. In Figure 3C, AN printed at a 50  $\mu\text{g}/\text{cm}^2$  concentration is shown, and in 3D AN printed a 5  $\mu\text{g}/\text{cm}^2$  concentration is shown. In Figure 3E, a typical SERS spectrum of AN at a 50  $\mu\text{g}/\text{cm}^2$  concentration is shown, main bands are located at 713  $\text{cm}^{-1}$  and 1044  $\text{cm}^{-1}$ . In the spectrum, the 1044  $\text{cm}^{-1}$  band observed corresponds with the symmetric stretch mode of  $\text{NO}_3^-$ .<sup>(20, 82)</sup> For data analysis, the main AN band at 1044  $\text{cm}^{-1}$  will be used for determining signal-to-noise (S/N) ratios.

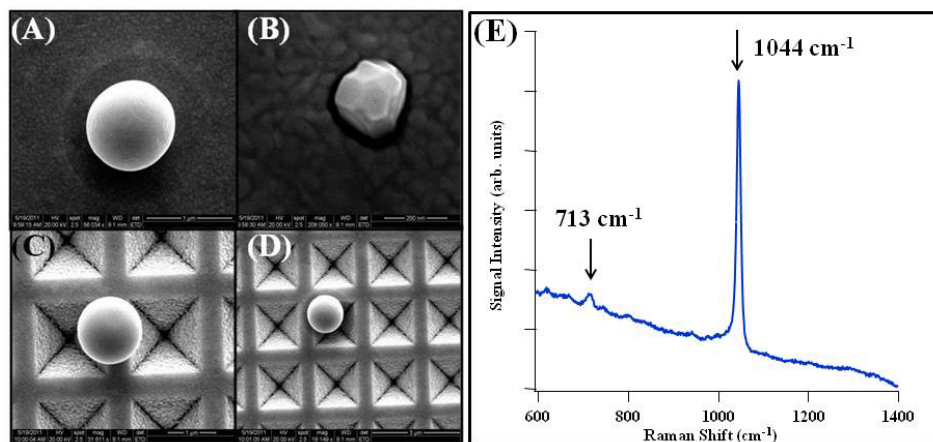


Figure 3. Example SEM images of ammonium nitrate deposited on a standard Klarite substrate. In (A) and (B) example physical difference in droplets observed are demonstrated. In (C) and (D) different concentrations of ammonium nitrate are deposited. In (E) a typical spectrum for AN is shown, main bands located at 713  $\text{cm}^{-1}$  and 1044  $\text{cm}^{-1}$ .

In Figure 4, data sets for AN deposited at different concentrations on Klarite substrates are shown. In Figure 4A, Raman and SERS data collected on a standard Klarite with AN concentrations of 5  $\mu\text{g}/\text{cm}^2$ , 20  $\mu\text{g}/\text{cm}^2$  and 50  $\mu\text{g}/\text{cm}^2$  are shown. This data was analyzed comparing the S/N ratio for the 1044  $\text{cm}^{-1}$  band of AN. From Figure 4A, it can be clearly seen that the SERS signal as compared to the Raman signal on a standard Klarite substrate is significantly greater. In Figure 4A, the 5  $\mu\text{g}/\text{cm}^2$  Raman S/N ratio is 2.02 and for SERS it is 38.75, 20  $\mu\text{g}/\text{cm}^2$  Raman S/N ratio is 5.48 and for SERS it is 67.50, and 50  $\mu\text{g}/\text{cm}^2$  Raman S/N ratio is 1.89 and for SERS it is 82.90. Thus it can be seen that the SERS signal is typically at least 19X greater than the Raman signal. Next, the detection capabilities of the standard Klarite and Klarite 308 were compared for trace levels of deposited AN. In Figure 4B, the SERS signal from AN deposited at 0.05  $\mu\text{g}/\text{cm}^2$  and 0.50  $\mu\text{g}/\text{cm}^2$  were compared on the two different SERS substrate types. For AN deposited at a concentration of 0.05  $\mu\text{g}/\text{cm}^2$ , the Raman S/N ratio is 1.24, the standard Klarite S/N ratio is 6.31, and the next generation Klarite 308 S/N ratio

is 17.28. This indicates that overall, the 308 is performing 2.73X better as compared to the standard commercial substrate. For AN deposited at a concentration of 0.50  $\mu\text{g}/\text{cm}^2$ , the Raman S/N ratio is 1.15, the standard Klarite S/N ratio is 9.03, and the next generation Klarite 308 S/N ratio is 32.17. This indicates that overall, the 308 is performing 3.6X better as compared to the standard commercial substrate. Thus indicating that for trace analysis, the next generation Klarite substrate performs better as compared to the standard Klarite substrate. With additional optimization, and the use of other energetic analytes, the overall signal increase with the next generation Klarite substrate may continue to improve.

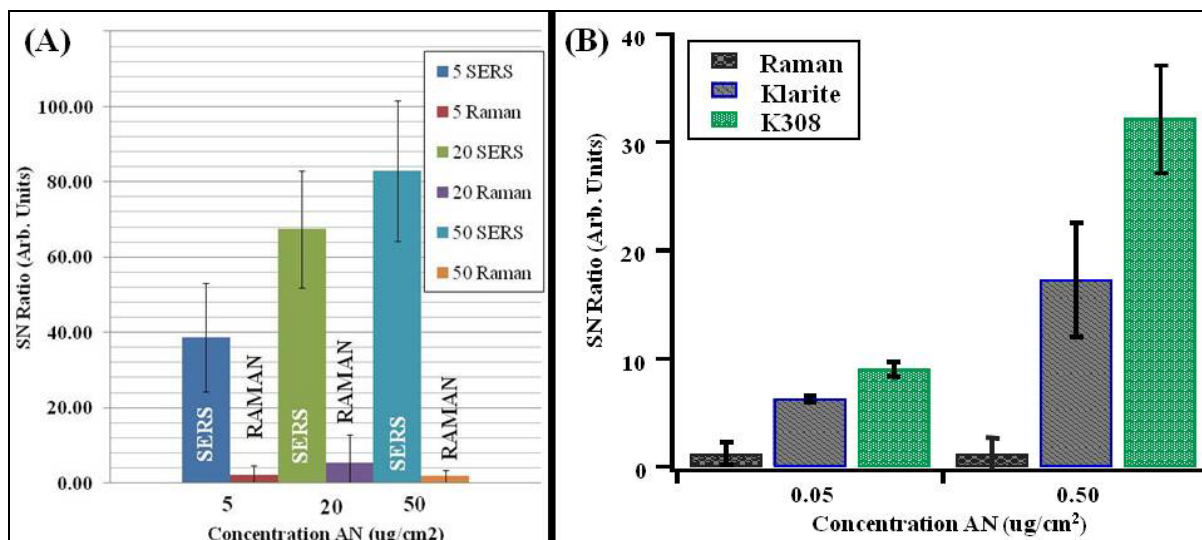


Figure 4. (A) S/N ratios for AN deposited at concentrations of 5, 20, and 50  $\mu\text{g}/\text{cm}^2$ . SERS and Raman data is shown. In (B) the S/N ratios for standard and next generation Klarite substrates shown for AN deposited at 0.05 and 0.50  $\mu\text{g}/\text{cm}^2$ .

Having successfully demonstrated the use of the standard and next generation substrates for sensing trace levels of IED components, we next demonstrated the applicability of using these substrates for detecting explosive samples. Explosives can be categorized as either primary or secondary based on how they are initiated. Primary explosives are typically detonated by some sort of ignition spark, and in some cases can be more challenging to handle. Secondary explosives require a detonator or primary explosive, and are typically characterized as being less sensitive to handling.<sup>(5)</sup> Some familiar examples of secondary explosives include RDX, PETN and TNT. Some of these secondary explosives can all be characterized as being very powerful and brisant.<sup>(83)</sup>

For these experiments, the energetic materials to be characterized with the commercial substrates include RDX, PETN, and TNT. These materials were microjetted onto standard Klarite substrates at a concentration of 5.0  $\mu\text{g}/\text{cm}^2$ . The concentration jetted was validated using a secondary UV-Vis technique.<sup>(20, 81)</sup> After jetting, the samples were stored covered until just prior to use. In Figure 5A-D example SEM images of the explosive material RDX deposited on a standard Klarite substrate are shown. From Figure 5A, the low magnification SEM image demonstrates how the drop spreads out across the standard Klarite substrate, resulting in a minor “coffee ring” effect. In Figure 5D, a higher magnification SEM image clearly demonstrates the spread of energetic materials across the features of the standard Klarite substrate. In Figure 5D, example SERS spectra from a 5.0  $\mu\text{g}/\text{cm}^2$  concentration of TNT, PETN and RDX as collected on individual standard Klarite substrate are shown. The explosive material TNT has SERS bands located at 793  $\text{cm}^{-1}$ , 823  $\text{cm}^{-1}$  ( $\text{NO}_2$  scissoring vibration), and 1356  $\text{cm}^{-1}$  ( $\text{NO}_2$  symmetric stretching coupled to CN stretching).<sup>(20)</sup> PETN has main SERS bands observed at 869  $\text{cm}^{-1}$  (ON stretch) and 1290  $\text{cm}^{-1}$  ( $\text{NO}_2$  symmetric stretch with some minor contributions from CH bending,  $\text{CH}_2$  wagging and  $\text{C}_5$  skeletal vibrations).<sup>(20)</sup> SERS bands for RDX are located at 877.4  $\text{cm}^{-1}$  (symmetric ring-breathing mode) and 1315  $\text{cm}^{-1}$  (NN stretch and  $\text{CH}_2$  twist).<sup>(20, 84)</sup> From Figure 5D, it is clear that all explosives materials have very distinct and identifiable SERS bands that can be measured using the standard Klarite SERS substrates.

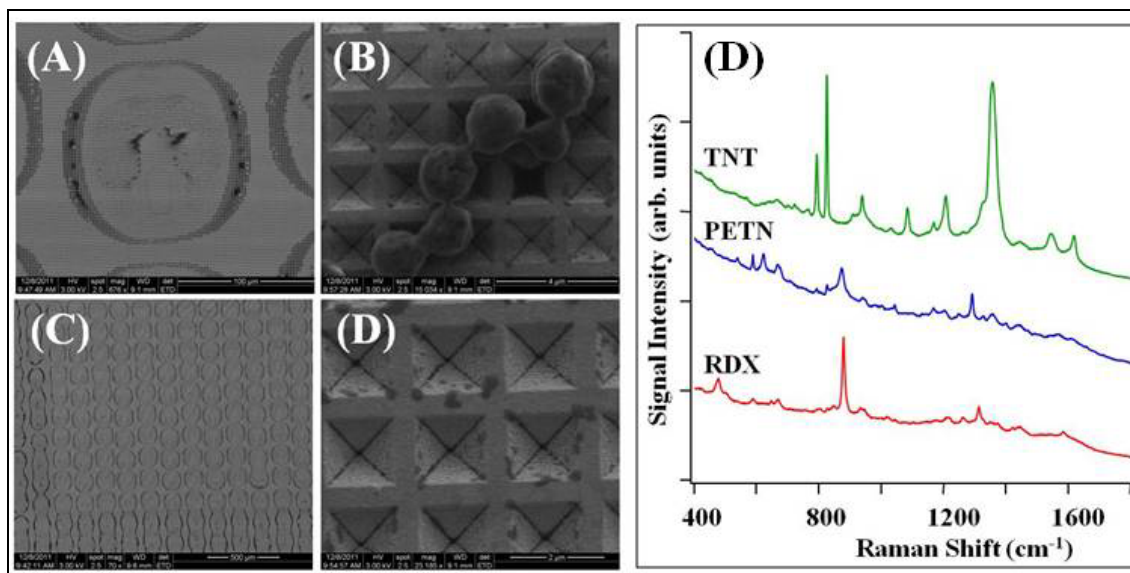


Figure 5. In (A-D) are example SEM images of RDX deposited on a standard Klarite substrate at different magnifications. In (E) example SERS spectra for common energetic samples TNT, PETN and RDX are shown.

Next, to demonstrate the potential for using the next generation Klarite substrates for SERS detection of low levels of energetic materials, the SERS spectra of the explosives TNT, PETN and RDX were collected. In these experiments the energetic materials were inkjetted onto different substrate surfaces at a concentration of 1  $\mu\text{g}/\text{cm}^2$ . For data analysis via a S/N ratio determination, the 1356  $\text{cm}^{-1}$  band of TNT, the 1290  $\text{cm}^{-1}$  band of PETN, and the 877.4  $\text{cm}^{-1}$  band of RDX were analyzed. In Figure 6A, example spectra for the energetic samples jetted onto the next generation Klarite substrate are shown. Bands used for S/N ratio determination are called out with a black arrow. In Figure 6B, the S/N ratios for the different energetic are shown (Raman and SERS measurements). From this data it was determined that at a 1  $\mu\text{g}/\text{cm}^2$  concentration the S/N ratio for TNT is  $150.0 \pm 22.5$  (Raman  $4.2 \pm 1.4$ ), for PETN is  $41.7 \pm 8.4$  (Raman  $8.1 \pm 1.0$ ), and for RDX is  $40.3 \pm 7.1$  (Raman  $3.6 \pm 9.4$ ). Analyzing this data it is determined that the next generation Klarite substrates can be used for the detection of low levels of energetic materials. Future work will determine the limits of detection possible with these substrates for energetic sensing.

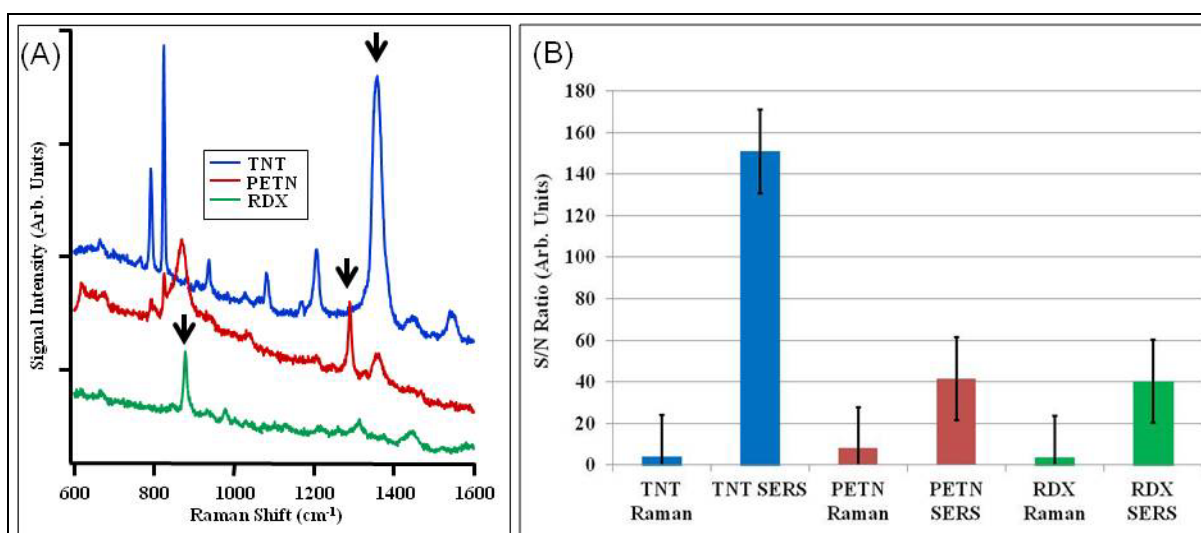


Figure 6. In (A) the spectra for TNT, PETN, and RDX as measured on the next generation Klarite 308 substrate. In (B) the S/N ratios for 1  $\mu\text{g}/\text{cm}^2$  of PETN and RDX inkjetted onto the active and nonactive areas of a next generation 308 Klarite substrate are shown.

#### IV. CONCLUSIONS

From the preliminary results shown, it can be concluded that the commercially available SERS substrates offer a viable approach for energetic detection at trace levels as demonstrated by detection of the common energetic hazards TNT, PETN, and RDX. Additionally, viability of detection of the common IED component AN was demonstrated. Future studies will include characterizing the response of the next generation Klarite substrates for trace samples of hazard materials.

#### ACKNOWLEDGEMENTS

Thank you to summer student Keely Tober for assistance with initial use of the MicroFab system summer 2009/ 2010. We also appreciate all assistance from MicroFab with system trouble shooting and the prompt installation of a new pressure controller.

#### REFERENCES

- [1] FAO, Current world fertilizer trends and outlook to 2011/12, in: C. Division (Ed.) FOOD AND AGRICULTURE ORGANIZATION OF THE UNITED NATIONS, Electronic Publishing Policy and Support Branch, Rome, Italy, 2008.
- [2] <http://en.wikipedia.org/wiki/ANFO>, ANFO in, Wikipedia, 2012.
- [3] [http://en.wikipedia.org/wiki/Oklahoma\\_City\\_bombing](http://en.wikipedia.org/wiki/Oklahoma_City_bombing), Oklahoma City bombing in, 2012.
- [4] Tom Vanden Brook, "IED attacks in Afghanistan set record," USA TODAY, (2012).
- [5] Sanders, K.P., Marshall, M., Oxley, J., Smith, J.L., Egee, L., "Preliminary investigation into the recovery of explosives from hair," Science & Justice, 137-142 (2002).
- [6] Oxley, J., Smith, J., Brady, J., Dubnikova, F., Kosloff, R., Zeiri, L., Zeiri, Y., "Raman and infrared fingerprint spectroscopy of peroxide-based explosives," Applied Spectroscopy, 906-915 (2008).
- [7] Gregory, O., Oxley, J., Smith, J., Platek, M., Ghonem, H., Bernier, E., Downey, M., Cumminskey, C., Sensors Surface Technology, P., "Microstructural characterization of pipe bomb fragments," Materials Characterization, 347-354 (2010).
- [8] Oxley, J., Smith, J.L., Brady, J., Naik, S., "Determination of Urea Nitrate and Guanidine Nitrate Vapor Pressures by Isothermal Thermogravimetry," Propellants Explosives Pyrotechnics, 278-283 (2010).
- [9] de Perre, C., Prado, A., McCord, B.R., "Rapid and specific detection of urea nitrate and ammonium nitrate by electrospray ionization time-of-flight mass spectrometry using infusion with crown ethers," Rapid Communications in Mass Spectrometry, 154-162 (2012).
- [10] Natan, A., Levitt, J.M., Graham, L., Katz, O., Silberberg, Y., "Standoff detection via single-beam spectral notch filtered pulses," Applied Physics Letters, (2012).
- [11] Ramin, S., Weller, M.G., "Extremely sensitive and selective antibodies against the explosive 2,4,6-trinitrotoluene by rational design of a structurally optimized hapten," Journal of Molecular Recognition, 89-97 (2012).
- [12] Upadhyayula, V.K.K., "Functionalized gold nanoparticle supported sensory mechanisms applied in detection of chemical and biological threat agents: A review," Analytica Chimica Acta, 1-18 (2012).
- [13] Wen, B., Eilers, H., "Potential interference mechanism for the detection of explosives via laser-based standoff techniques," Applied Physics B-Lasers and Optics, 473-482 (2012).
- [14] Rose, T.A., Smith, P.D., Mays, G.C., "Design charts relating to protection of structures against airblast from high explosives," Proceedings of the Institution of Civil Engineers-Structures and Buildings, 186-192 (1997).
- [15] Moore, D.S., "Instrumentation for trace detection of high explosives," Review of Scientific Instruments, 2499-2512 (2004).
- [16] Hoffman, B., "The 'cult of the insurgent': its tactical and strategic implications," Australian Journal of International Affairs, 312-329 (2007).
- [17] Wallin, S., Pettersson, A., Ostmark, H., Hobro, A., "Laser-based standoff detection of explosives: a critical review," Analytical and Bioanalytical Chemistry, 259-274 (2009).

- [18] Izake, E.L., "Forensic and homeland security applications of modern portable Raman spectroscopy," *Forensic Science International*, 1-8 (2010).
- [19] Scaffidi, J.P., Gregas, M.K., Lauly, B., Carter, J.C., Angel, S.M., Vo-Dinh, T., "Trace Molecular Detection via Surface-Enhanced Raman Scattering and Surface-Enhanced Resonance Raman Scattering at a Distance of 15 Meters," *Applied Spectroscopy*, 485-492 (2010).
- [20] Tuschel, D.D., Mikhonin, A.V., Lemoff, B.E., Asher, S.A., "Deep Ultraviolet Resonance Raman Excitation Enables Explosives Detection," *Applied Spectroscopy*, 425-432 (2010).
- [21] Ostmark, H., Nordberg, M., Carlsson, T.E., "Stand-off detection of explosives particles by multispectral imaging Raman spectroscopy," *Applied Optics*, 5592-5599 (2011).
- [22] Zachhuber, B., Gasser, C., Chrysostom, E.T.H., Lendl, B., "Stand-Off Spatial Offset Raman Spectroscopy for the Detection of Concealed Content in Distant Objects," *Analytical Chemistry*, 9438-9442 (2011).
- [23] Zachhuber, B., Ramer, G., Hobro, A., Chrysostom, E.T.H., Lendl, B., "Stand-off Raman spectroscopy: a powerful technique for qualitative and quantitative analysis of inorganic and organic compounds including explosives," *Analytical and Bioanalytical Chemistry*, 2439-2447 (2011).
- [24] Bantz, K.C., Meyer, A.F., Wittenberg, N.J., Im, H., Kurtulus, O., Lee, S.H., Lindquist, N.C., Oh, S.H., Haynes, C.L., "Recent progress in SERS biosensing," *Physical Chemistry Chemical Physics*, 11551-11567 (2011).
- [25] Fleischmann, M., Hendra, P.J., McQuillan, A.J., *Chem. Phys. Lett.*, 163-166 (1974).
- [26] Jeanmaire, D.L., Vanduyne, R.P., "Surface Raman Spectroelectrochemistry. 1. Heterocyclic, Aromatic, and Aliphatic-Amines Adsorbed on Anodized Silver Electrode," *J. Electroanal. Chem.*, 1 (1977).
- [27] Albrecht, M.G., Creighton, J.A., "Anomalous Intense Raman-Spectra of Pyridine at a Silver Electrode," *J. Am. Chem. Soc.*, 5215 (1977).
- [28] Dornhaus, R., Benner, R.E., Chang, R.K., Chabay, I., "Surface-plasmon contribution to SERS," *Surface Science*, 367-373 (1980).
- [29] Kerker, M., Siiman, O., Bumm, L.A., Wang, D.S., "Surface enhanced Raman-scattering (SERS) of citrate ion adsorbed on colloidal silver," *Applied Optics*, 3253-3255 (1980).
- [30] Kerker, M., Wang, D.S., Chew, H., "Surface enhanced Raman-scattering (SERS) by molecules adsorbed at spherical particles," *Applied Optics*, 3373-3388 (1980).
- [31] Wang, D.S., Chew, H., Kerker, M., "Enhanced Raman scattering at the surface (SERS) of a spherical particle," *Applied Optics*, 2256-2257 (1980).
- [32] Kneipp, K., Kneipp, H., Dasari, R.R., Feld, M.S., "Single molecule Raman spectroscopy using silver and gold nanoparticles," *Indian Journal of Physics and Proceedings of the Indian Association for the Cultivation of Science-Part B*, 39-47 (2003).
- [33] Campion, A., Kambhampati, P., "Surface-enhanced Raman scattering," *Chemical Society Reviews*, 241-250 (1998).
- [34] Cotton, T.M., Kim, J.H., Chumanov, G.D., "Application of surface-enhanced Raman spectroscopy to biological systems," *Journal of Raman Spectroscopy*, 729-742 (1991).
- [35] Kneipp, K., Kneipp, H., Itzkan, I., Dasari, R.R., Feld, M.S., "Surface-enhanced Raman scattering and biophysics," *Journal of Physics-Condensed Matter*, R597-R624 (2002).
- [36] Baker, G.A., Moore, D.S., "Progress in plasmonic engineering of surface-enhanced Raman-scattering substrates toward ultra-trace analysis," *Analytical and Bioanalytical Chemistry*, 1751-1770 (2005).
- [37] Yonzon, C.R., Stuart, D.A., Zhang, X.Y., McFarland, A.D., Haynes, C.L., Van Duyne, R.P., "Towards advanced chemical and biological nanosensors - An overview," *Talanta*, 438-448 (2005).
- [38] Willets, K.A., Van Duyne, R.P., "Localized surface plasmon resonance spectroscopy and sensing," in: *Annual Review of Physical Chemistry*, 2007, pp. 267-297.
- [39] Banholzer, M.J., Millstone, J.E., Qin, L.D., Mirkin, C.A., "Rationally designed nanostructures for surface-enhanced Raman spectroscopy," *Chemical Society Reviews*, 885-897 (2008).
- [40] Kneipp, J., Kneipp, H., Kneipp, K., "SERS - a single-molecule and nanoscale tool for bioanalytics," *Chemical Society Reviews*, 1052-1060 (2008).

- [41] Qian, X.M., Nie, S.M., "Single-molecule and single-nanoparticle SERS: from fundamental mechanisms to biomedical applications," *Chemical Society Reviews*, 912-920 (2008).
- [42] Stiles, P.L., Dieringer, J.A., Shah, N.C., Van Duyne, R.R., Surface-Enhanced Raman Spectroscopy, in: *Annual Review of Analytical Chemistry*, 2008, pp. 601-626.
- [43] Qian, X.M., Peng, X.H., Ansari, D.O., Yin-Goen, Q., Chen, G.Z., Shin, D.M., Yang, L., Young, A.N., Wang, M.D., Nie, S.M., "In vivo tumor targeting and spectroscopic detection with surface-enhanced Raman nanoparticle tags," *Nature Biotechnology*, 83-90 (2008).
- [44] Li, H., Baum, C.E., Cullum, B.M., "Characterization of novel Gold SERS Substrates with Multilayer Enhancements," *SPIE*, (2006).
- [45] Li, H., Baum, C.E., Sun, J., Cullum, B.M., "Multilayer enhanced SERS active materials: fabrication, characterization, and application to trace chemical detection," *SPIE*, 621804 (2006).
- [46] Li, H., Patel, P.H., Cullum, B.M., "Novel multilayered SERS substrates for trace chemical and biochemical analysis," *SPIE*, (2004).
- [47] Vo-Dinh, T., Cullum, B.M., Stokes, D.L., Nanosensors and biochips: frontiers in biomolecular diagnostics, in, *Elsevier Science Sa*, 2001, pp. 2-11.
- [48] Hankus, M.E., Cullum, B.M., "SERS probes for the detection and imaging of biochemical species on the nanoscale," *Proceedings of the SPIE - The International Society for Optical Engineering*, 638004-638001-638012 (2006).
- [49] Cao, Y.W.C., Jin, R.C., Mirkin, C.A., "Nanoparticles with Raman Spectroscopic Fingerprints for DNA and RNA Detection," *Science*, 1536 (2002).
- [50] Chowdhury, M.H., Gant, V.A., Trache, A., Baldwin, A., Meininger, G.A., Cote, G.L., "Use of surface-enhanced Raman spectroscopy for the detection of human integrins," *Journal of Biomedical Optics*, 8 (2006).
- [51] Culha, M., Adiguzel, A., Yazici, M.M., Kahraman, M., Sahin, F., Gulluce, M., "Characterization of Thermophilic Bacteria Using Surface-Enhanced Raman Scattering," *Applied Spectroscopy*, 1226-1232 (2008).
- [52] Jarvis, R.M., Law, N., Shadi, I.T., O'Brien, P., Lloyd, J.R., Goodacre, R., "Surface-Enhanced Raman Scattering from Intracellular and Extracellular Bacterial Locations," *Analytical Chemistry*, 6741-6746 (2008).
- [53] Tripp, R.A., Dluhy, R.A., Zhao, Y.P., "Novel nanostructures for SERS biosensing," *Nano Today*, 31-37 (2008).
- [54] Driskell, J.D., Shanmukh, S., Liu, Y.J., Hennigan, S., Jones, L., Zhao, Y.P., Dluhy, R.A., Krause, D.C., Tripp, R.A., "Infectious agent detection with SERS-active silver nanorod arrays prepared by oblique angle deposition," *IEEE Sensors Journal*, 863-870 (2008).
- [55] Holthoff, E.L., Stratis-Cullum, D.N., Hankus, M.E., "A Nanosensor for TNT Detection Based on Molecularly Imprinted Polymers and Surface Enhanced Raman Scattering," *Sensors*, 2700-2714 (2011).
- [56] Holthoff, E.L., Stratis-Cullum, D.N., Hankus, M.E., "Xerogel-Based Molecularly Imprinted Polymers for Explosives Detection," *Chemical, Biological, Radiological, Nuclear, and Explosives (Cbrne) Sensing Xi*, (2010).
- [57] Norrod, K.L., Sudnik, L.M., Rousell, D., Rowlen, K.L., "Quantitative Comparison of Five SERS Substrates: Sensitivity and Limit of Detection," *Appl. Spectros.*, 994 (1997).
- [58] Alexander, T.A., Le, D.M., "Characterization of a commercialized SERS-active substrate and its application to the identification of intact *Bacillus endospores*," *Appl. Opt.*, (2007).
- [59] Guicheteau, J., Christesen, S., Emge, D., Wilcox, P., Fountain, A.W., III, "Assessing Metal Nanofabricated Substrates for Surface-Enhanced Raman Scattering (SERS) Activity and Reproducibility," *Applied Spectroscopy*, 144-151 (2011).
- [60] Kneipp, K., Kneipp, H., Itzkan, I., Dasari, R.R., Feld, M.S., "Surface-enhanced Raman scattering: A new tool for biomedical spectroscopy," *Current Science*, 915-924 (1999).
- [61] Jones, J.P., Fell, N.F., Alexander, T., Fountain, A.W., "Photonic Nanostructures as SERS Substrates for Reproducible Characterization of Bacterial Spores," *SPIE*, 94-104 (2004).
- [62] Kneipp, H., Kneipp, K., "Surface-enhanced hyper Raman scattering in silver colloidal solutions," *Journal of Raman Spectroscopy*, 551-554 (2005).
- [63] Kao, P., Malvadkar, N.A., Cetinkaya, M., Wang, H., Allara, D.L., Demirel, M.C., "Surface-enhanced Raman detection on metalized nanostructured poly(p-xylylene) films," *Advanced Materials*, 3562-+ (2008).



- [64] Becker, M., Sivakov, V., Goesele, U., Stelzner, T., Andra, G., Reich, H.J., Hoffmann, S., Michler, J., Christiansen, S.H., "Nanowires enabling signal-enhanced nanoscale Raman spectroscopy," *Small*, 398-404 (2008).
- [65] Xie, J., Zhang, Q., Lee, J.Y., Wang, D.I.C., "The Synthesis of SERS-Active Gold Nanoflower Tags for In Vivo Applications," *ACS Nano*, 2473-2480 (2008).
- [66] Braun, G., Pavel, I., Morrill, A.R., Seferos, D.S., Bazan, G.C., Reich, N.O., Moskovits, M., "Chemically Patterned Microspheres for Controlled Nanoparticle Assembly in the Construction of SERS Hot spots," *J. Am. Chem. Soc.*, 7760-7761 (2007).
- [67] Kho, K.W., Shen, Z.X., Zeng, H.C., Soo, K.C., Olivo, M., "Deposition Method for Preparing SERS-Active Gold Nanoparticle Substrates," *Analytical Chemistry*, 7462-7471 (2005).
- [68] Jian, S., Hankus, M.E., Cullum, B.M., "SERS based immuno-microwell arrays for multiplexed detection of foodborne pathogenic bacteria," *Proceedings of the SPIE - The International Society for Optical Engineering*, 73130K (73110 pp.) (2009).
- [69] Hankus, M.E., Gibson, G., Chandrasekharan, N., Cullum, B.M., "Surface-enhanced Raman scattering (SERS) - nanoimaging probes for biological analysis," *Smart Medical and Biomedical Sensor Technology II*, 106-116 (2004).
- [70] Kuncicky, D.M., Prevo, B.G., Velev, O.D., "Controlled assembly of SERS substrates templated by colloidal crystal films," *J. Mater. Chem.*, 1207-1211 (2006).
- [71] Kneipp, K., Kneipp, H., Kneipp, J., "Surface-enhanced Raman scattering in local optical fields of silver and gold nanoaggregates - From single-molecule Raman spectroscopy to ultrasensitive probing in live cells," *Accounts of Chemical Research*, 443-450 (2006).
- [72] Lee, C.H., Hankus, M.E., Tian, L., Pellegrino, P.M., Singamaneni, S., "Highly Sensitive SERS Substrates Based on Filter Paper Loaded with Plasmonic Nanostructures," *Anal. Chem.*, (2011).
- [73] Alexander, T.A., "Applications of Surface-Enhanced Raman Spectroscopy (SERS) for Biosensing: An Analysis of Reproducible, Commercially Available Substrates," *SPIE*, 600703 (2005).
- [74] Alexander, T.A., "Development of Methodology Based on commercialized SERS-active Substrates for Rapid Discrimination of Poxviridae Virions," *Anal. Chem.*, 2817-2825 (2008).
- [75] Alexander, T.A., Pellegrino, P.M., Gillespie, J.B., "Near-Infrared Surface-Enhanced-Raman-Scattering-Mediated Detection of Single Optically Trapped Bacterial Spores," *Applied Spectroscopy*, 1340-1345 (2003).
- [76] Netti, M.C., Zoorob, M.E., Charlton, M.C.B., Ayliffe, P., Mahnkopf, S., Stopford, P., Todd, K., Lincoln, J.R., Perney, N.M.B., Baumberg, J.J., "Probing molecules by Surface-Enhanced Raman Spectroscopy," *SPIE*, (2006).
- [77] Hankus, M., Stratis-Cullum, D., Pellegrino, P., "Enabling Technologies for Point and Remote Sensing of Chemical and Biological Agents Using Surface Enhanced Raman Scattering (SERS) Techniques," *ARL Technical Report*, 132 (2009).
- [78] Hankus, M.E., Stratis-Cullum, D.N., Pellegrino, P.M., "Characterization of next-generation commercial surface-enhanced Raman scattering (SERS) substrates," *Proc. SPIE*, 80180P (2011).
- [79] Hankus, M.E., Stratis-Cullum, D.N., Pellegrino, P.M., "Surface enhanced Raman scattering (SERS)-based next generation commercially available substrate: physical characterization and biological application," *Proceedings of the SPIE - The International Society for Optical Engineering*, (2011).
- [80] Holthoff, E.L., Hankus, M.E., Pellegrino, P.M., "Investigating a drop-on-demand microdispenser for standardized sample preparation," *Proc. SPIE - Int. Soc. Opt. Eng.*, 80181F-80190F (2011).
- [81] Emmons, E.D., Farrell, M.E., Holthoff, E.L., Tripanthi, A., Green, N., Moon, R.P., Guicheateau, J.A., D.Christesen, S., Pellegrino, P.M., III, A.W.F., "Characterization of Polymorphic States in Energetic Samples of 1,3,5-Trinitro-1,3,5-Triazine (RDX) Fabricated Using Drop-on-Demand Inkjet Technology," *Applied Spectroscopy*, (2012).
- [82] Owens, F.J., "Reproducible surface-enhanced Raman spectroscopy of small molecular anions," *Molecular Physics*, 667-671 (2011).
- [83] McNesby, K.L., Fell, N.F., Vanderhoff, J.A., "Detection and Characterization of Explosives Using Raman Spectroscopy: Identification, Laser heating, and Impact Sensitivity," *SPIE*, 121-135 (1997).
- [84] Torres, P., Mercado, L., Cotte, I., Hernadez, S.P., Mina, N., Santana, A., Chamberlain, R.T., Lareau, R., Castro, M.E., "Vibrational Spectroscopy Study of B and A RDX Deposits," *J. Phys. Chem. B*, 8799-8805 (2004).

DEFENSE TECH INFO CTR  
ATTN DTIC OCA (PDF)  
8725 JOHN J KINGMAN RD STE 0944  
FT BELVOIR VA 22060-6218

US ARMY RSRCH LAB  
ATTN IMAL HRA MAIL & RECORDS MGMT  
ATTN RDRL CIO LL TECHL LIB  
ATTN RDRL CIO LT TECHL PUB  
ATTN RDRL SEE E M FARRELL (3 COPIES)  
ADELPHI MD 20783-1197